

# Candidate autism gene screen identifies critical role for cell-adhesion molecule CASPR2 in dendritic arborization and spine development

Garret R. Anderson<sup>a,b</sup>, Timothy Galfin<sup>a,b</sup>, Wei Xu<sup>a,c</sup>, Jason Aoto<sup>a</sup>, Robert C. Malenka<sup>b</sup>, and Thomas C. Südhof<sup>a,c,1</sup>

<sup>a</sup>Department of Molecular and Cellular Physiology, <sup>b</sup>Nancy Pritzker Laboratory, Department of Psychiatry and Behavioral Sciences, and <sup>c</sup>Howard Hughes Medical Institute, Stanford University School of Medicine, Stanford, CA 94305

Contributed by Thomas C. Südhof, September 19, 2012 (sent for review August 2, 2012)

**Mutations in the contactin-associated protein 2 (*CNTNAP2*) gene encoding CASPR2, a neurexin-related cell-adhesion molecule, predispose to autism, but the function of CASPR2 in neural circuit assembly remains largely unknown. In a knockdown survey of autism candidate genes, we found that CASPR2 is required for normal development of neural networks. RNAi-mediated knockdown of CASPR2 produced a cell-autonomous decrease in dendritic arborization and spine development in pyramidal neurons, leading to a global decline in excitatory and inhibitory synapse numbers and a decrease in synaptic transmission without a detectable change in the properties of these synapses. Our data suggest that in addition to the previously described role of CASPR2 in mature neurons, where CASPR2 organizes nodal microdomains of myelinated axons, CASPR2 performs an earlier organizational function in developing neurons that is essential for neural circuit assembly and operates coincident with the time of autism spectrum disorder (ASD) pathogenesis.**

dendrite | synaptogenesis

Autism spectrum disorders (ASDs) comprise a heterogeneous group of early developmental diseases characterized by repetitive and stereotypic behaviors and impairments in social interactions and language development. ASDs are highly heritable, with recent studies linking mutations at hundreds of genes to ASDs (1–3). These findings raised the fundamental question of how these genes might act in neural circuits without being essential for all brain function. Here, we have attempted to address this question by using a Ca<sup>2+</sup>-imaging screening platform to visualize changes in excitatory network activity following shRNA-mediated knockdown (KD) of prominent cell-adhesion molecules that have been repeatedly implicated in the development of ASDs. We found that molecular manipulation of several ASD candidate genes profoundly influences network activity as monitored by this assay. We observed the biggest effects with the neuronal cell-adhesion molecule contactin-associated protein 2 (CASPR2) that is encoded by the *CNTNAP2* gene, leading us to specifically focus on the mechanisms by which this cell-adhesion molecule influences neural circuit development.

Mutations in the *CNTNAP2* gene have been repeatedly identified in ASD patients (for review, see ref. 4). In addition, mutations in *CNTNAP2* also have been linked to epilepsy (5–7), Tourette syndrome (8, 9), schizophrenia (5, 7, 10), attention deficit hyperactivity disorder (ADHD) (11), learning disability (12, 13), and language impairment (14–16). Thus, *CNTNAP2* is of central importance for human brain function, as additionally shown by recent *in vivo* MRI studies in which variations in the *CNTNAP2* gene were associated with reduced frontal gray matter and altered functional connectivity (17, 18).

CASPR2 is a member of the contactin-associated protein family (19). CASPRs are referred to as neurexin IV in *Drosophila* and are highly homologous to neuexins, which are presynaptic cell-adhesion molecules (20–23). CASPR2 is best known for its role in myelinated axons, where it localizes to juxtaparanodal regions and forms a complex with contactin 2 (CNTN2) to generate a membrane scaffold that clusters Kv1 channels (reviewed in refs. 24 and 25). Knockout of CASPR2 in mice results in epilepsy and behavioral

abnormalities that are consistent with the symptoms observed in some cases of ASDs (26, 27). The loss of CASPR2 in neurons, however, not only depletes K<sup>+</sup> channels from myelinated juxtaparanodal regions (26, 27) but also causes a 20% reduction in the number of interneurons in cortex, hippocampus, and striatum, as well as discrete alterations in neuronal migration and cortical layer patterning (26). Most of these phenotypic features cannot be explained by a dysfunction of myelinated nerves, suggesting that CASPR2 performs additional functions besides organizing axonal subdomains. Consistent with this idea, CASPR2 is expressed early in brain development before myelination and is abundantly present in gray matter of adult brain in which myelin is not as abundant as in white matter (19). Moreover, the homology of CASPR2 to neuexins suggests a possible role in synapse formation and/or function or in other neuronal cell-adhesion processes, although such a role has not yet been investigated.

To explore the function of CASPR2 in developing neurons before myelination, we examined the role of CASPR2 in cortical neurons cultured from newborn mice, using a KD and rescue approach. Our studies demonstrate a cell-autonomous function of CASPR2 in controlling the arborization of dendrites and the maturation of dendritic spines. Loss of this function indirectly impairs synapse formation and neural network assembly, leading to a global decrease of synaptic transmission. Our data provide a potential explanation for the role of CASPR2 mutations in ASDs and epilepsy that manifests before most myelination occurs.

## Results

**CASPR2 KD Suppresses Neural Network Activity.** Multiple cell-adhesion molecules were identified as ASD candidate genes in large-scale genomic analyses (Table S1). To evaluate the potential role of these molecules in neurons, we first established a Ca<sup>2+</sup>-imaging approach to measure Ca<sup>2+</sup> transients during neural network activity in neurons cultured from mouse cortex (Fig. 1A–C).

We loaded cultured cortical neurons with the membrane-permeable fluorescent Ca<sup>2+</sup> indicator Fluo-4 acetoxyethyl ester (AM) and induced neural network activity by addition of the GABA<sub>A</sub>-receptor antagonist picrotoxin (50 μM; Fig. 1A and B). The dendritic and somatic Ca<sup>2+</sup> transients in neurons firing action potentials during picrotoxin-induced network activity were blocked by addition of antagonists of voltage-gated sodium channels (tetrodotoxin; 0.5 μM) or of NMDA-type (AP5; 50 μM) or AMPA-type (CNQX; 20 μM) glutamate receptors, indicating that the Ca<sup>2+</sup> transients were both depolarization- and glutamate receptor-dependent (Fig. 1C).

We then tested whether our Ca<sup>2+</sup>-imaging approach was sufficiently sensitive to detect changes in synaptic transmission induced

Author contributions: G.R.A., T.G., W.X., J.A., R.C.M., and T.C.S. designed research; G.R.A., T.G., W.X., and J.A. performed research; G.R.A., T.G., W.X., J.A., and T.C.S. analyzed data; and G.R.A., R.C.M., and T.C.S. wrote the paper.

The authors declare no conflict of interest.

<sup>1</sup>To whom correspondence should be addressed. E-mail: tcs1@stanford.edu.

This article contains supporting information online at [www.pnas.org/lookup/suppl/doi:10.1073/pnas.1216398109/-DCSupplemental](http://www.pnas.org/lookup/suppl/doi:10.1073/pnas.1216398109/-DCSupplemental).

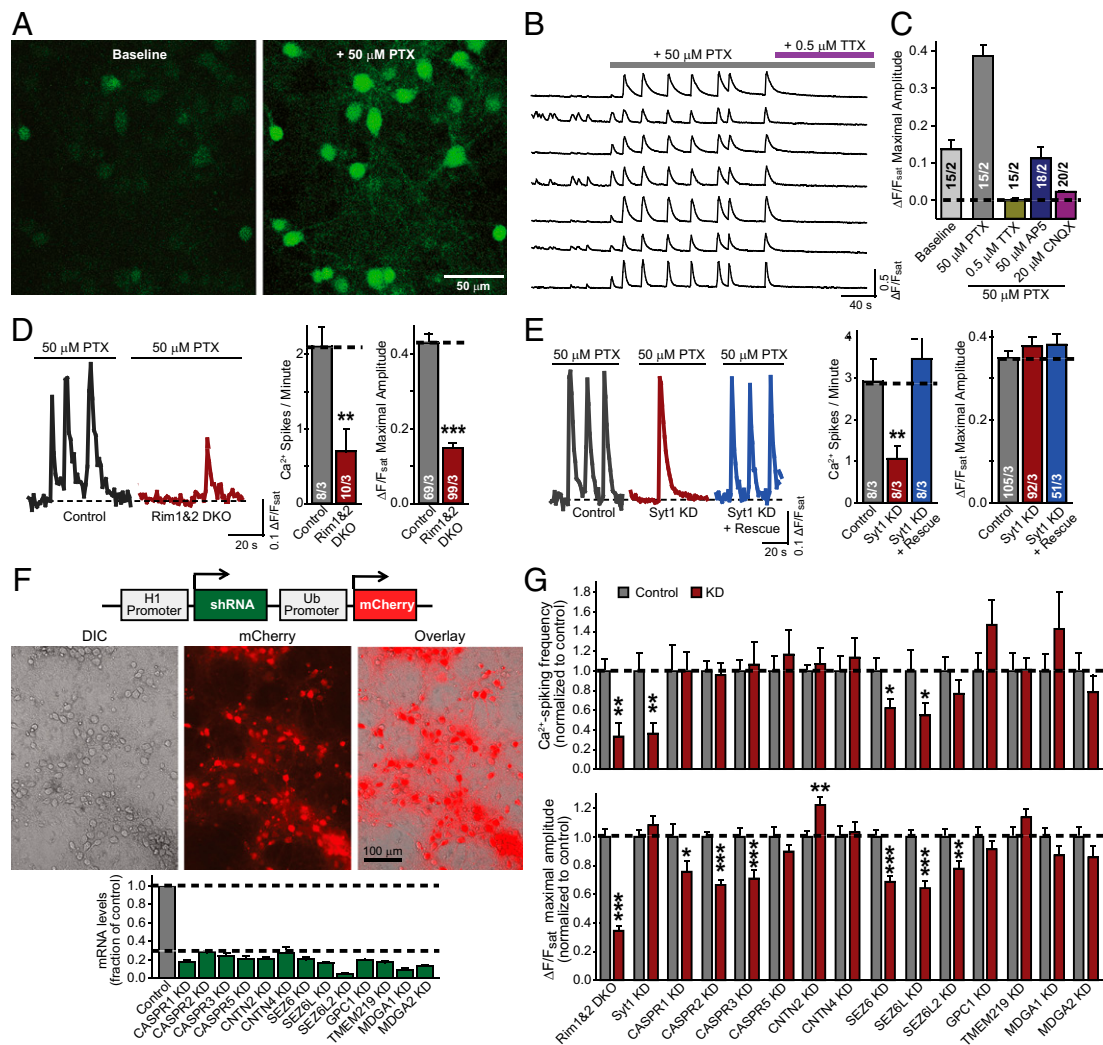


**Fig. 1.** Autism gene survey identifies CASPR2 function in maintaining normal neural network activity. (A) Representative image of cultured cortical neurons loaded with the  $\text{Ca}^{2+}$  indicator Fluo-4 AM, under basal resting conditions (Left) and upon addition of  $50 \mu\text{M}$  picrotoxin (PTX) to elicit large spontaneous transient increases in fluorescence intensity (Right). (B and C) Sample traces (B) and summary graphs (C) of spontaneous somatic  $\text{Ca}^{2+}$  transients monitored in cultured cortical neurons before and after treatment with  $50 \mu\text{M}$  picrotoxin, followed by coapplication of  $0.5 \mu\text{M}$  TTX,  $50 \mu\text{M}$  AP5, or  $20 \mu\text{M}$  CNQX to silence picrotoxin induced network activity. (D and E) Validation of  $\text{Ca}^{2+}$ -imaging analysis of neural network activity. Sample traces (Left) and summary graphs (Right) of somatic  $\text{Ca}^{2+}$  transients were monitored in cultured cortical neurons from conditional RIM1/2 double KO neurons that were infected with lentiviruses expressing inactive (Control) or active cre-recombinase (RIM1&2 DKO) (D) or wild-type neurons infected with a control lentivirus (control) or lentiviruses expressing an shRNA to synaptotagmin-1 alone (Syt1 KD) or together with a synaptotagmin-1 rescue cDNA (Syt1 KD + rescue) (E). (F) Design of the lentiviral vector (L309) expressing shRNAs under the control of H1 promoter and mCherry under the control of ubiquitin (Ub) promoter (Top), representative images of cultured cortical neurons after lentiviral expression of mCherry (Middle), and measurements of the mRNA KD efficiency obtained for the indicated targets (Bottom). (G) Cultured cortical neurons were infected with control lentiviruses and lentiviruses knocking down the indicated genes, and picrotoxin induced network activity in the infected neurons was analyzed by Fluo-4  $\text{Ca}^{2+}$  imaging. Both the frequency of  $\text{Ca}^{2+}$  transients (Upper) and maximal amplitudes (Lower) were evaluated. Data shown are means  $\pm$  SEMs (for C, D, and E, number of cells/independent cultures analyzed are depicted in the bars; for F,  $n = 2-4$  cultures; for G, for the  $\text{Ca}^{2+}$  spikes/min graphs,  $n = 8-14$  fields of view/3-5 independent cultures, and for the data shown in the  $\Delta\text{F}/\text{F}_{\text{sat}}$  maximal amplitude graphs,  $n = 50-186$  neurons/3-5 independent cultures). Statistical significance was evaluated by Student's *t* test comparing the various test conditions to their respective control ( $*P < 0.05$ ;  $**P < 0.01$ ;  $***P < 0.001$ ).

by alterations in synaptic proteins. For this purpose, we evaluated synaptic network activity in neurons lacking the presynaptic active zone proteins RIM1 and RIM2 (Fig. 1D) or the synaptic vesicle protein synaptotagmin-1 (Fig. 1E). Losses of RIMs or of synaptotagmin-1, which cause distinct phenotypes as examined by electrophysiology (28–30), produced distinct changes in neural network activity. These changes manifested as different alterations of the frequencies and amplitudes of picrotoxin-elicited  $\text{Ca}^{2+}$  transients, confirming the utility of the approach.

We next screened multiple shRNAs for a given target cell-adhesion molecule by expressing the shRNAs in cultured cortical neurons. We measured the levels of the endogenous mRNAs by

quantitative RT-PCR to avoid artifacts attributable to the use of reporter constructs in nonneuronal cells. We selected shRNAs that suppress target mRNAs by  $>70\%$  (Fig. 1F and Tables S2–S4) and tested the effects of these shRNAs on neural network activity as visualized by  $\text{Ca}^{2+}$  imaging (Fig. 1G). Using this approach, we identified several ASD-implicated neuronal cell-adhesion molecules whose KD altered neuronal network activity. Notably, we observed alterations upon KD of members of the seizure-related gene 6 family (SEZ6, SEZ6L, and SEZ6L2) and the CASPR family (CASPR1, CASPR2, and CASPR3).

SEZ6 was previously shown to affect excitatory synaptic transmission (31), which, here, we observed not only with SEZ6 but

also with SEZ6L and SEZ6L2. Similar to the SEZ6 proteins, we detected a decrease in  $\text{Ca}^{2+}$  signals upon KD of CASPR proteins, with the most prominent suppression observed upon KD of CASPR2. Furthermore, our screen included the CASPR2-ligand contactin-2 (CNTN2), whose KD altered  $\text{Ca}^{2+}$  signals during network activity in a pattern that was opposite to the effect observed with the CASPR2 KD (Fig. 1G). Thus, we decided to focus on CASPR2 and CNTN2 to investigate their bidirectional effect on synaptic signaling in a neural network. Because KDs frequently suffer from substantial off-target effects (32), we validated the CASPR2 and CNTN2 KD phenotypes we observed by rescuing these phenotypes with shRNA-resistant cDNAs.

Detailed analyses of the CASPR2 KD revealed that it decreased the amplitude of  $\text{Ca}^{2+}$  signals during network activity without altering the frequency of  $\text{Ca}^{2+}$  spikes or their kinetics. This phenotype was rescued by expression of a KD-resistant CASPR2 cDNA (Fig. 2A and B). Electrophysiological recordings of excitatory postsynaptic currents (EPSCs) showed that the

total charge transfer of synaptic responses during network activity, but not the frequency of EPSC bursts, was dramatically decreased by the CASPR2 KD, confirming that the  $\text{Ca}^{2+}$ -imaging phenotype faithfully reflected a change in neural network activity produced by the CASPR2 KD (Fig. 2C and D).

Strikingly, KD of contactin-2, a CASPR2 ligand for which CASPR was originally named (33), produced a phenotype opposite to that of the CASPR2 KD: an increase in the amplitude of  $\text{Ca}^{2+}$  signals attributable to a decrease in the decay of  $\text{Ca}^{2+}$  signals, again without a change in the frequency of  $\text{Ca}^{2+}$  spikes (Fig. 2E and F). Similar to the CASPR2 KD effects, the contactin-2 KD effects were fully rescued by expression of shRNA-resistant contactin-2 cDNA (Fig. 2E and F). Taking together, these bidirectional effects suggest that CASPR2 and contactin-2 have at least partly nonoverlapping functions. Given that mutations in the *CNTNAP2* gene have repeatedly been identified in ASD patients (for review, see ref. 4), we proceeded to investigate and characterize in detail the functional role of CASPR2 that underlies the effects we observe here.

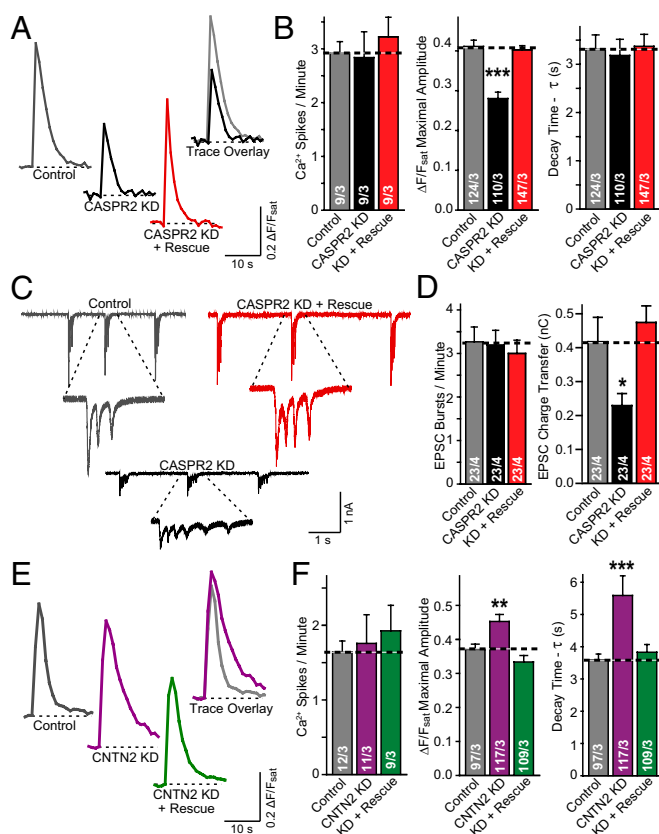


**Fig. 2.** CASPR2 and CNTN2 KD bidirectional effects on excitatory network activity is restored upon coexpression of rescue control. (A and B) Example (A) and summary (B) graphs of somatic  $\text{Ca}^{2+}$  transients monitored in cultured neurons infected with control lentivirus (Control) or lentiviruses expressing the CASPR2 shRNA without (CASPR2 KD) or with the CASPR2 rescue cDNA (KD + Rescue). (B) Frequency (Left), amplitude (Center), and decay time constants (Right) of  $\text{Ca}^{2+}$  signals as assessed with the  $\text{Ca}^{2+}$  indicator dye Fluo4-AM were quantified. (C and D) Sample (C) and summary (D) graphs of the frequency (Left) and magnitude (quantified as synaptic charge transfer) (Right) of spontaneous EPSC bursts measured during picROTOXIN-induced neuronal network activity in neurons obtained as described for A and B. (E and F) Same as A and B, except that the neurons were infected with control lentiviruses (Control) or lentiviruses expressing the contactin-2 KD shRNA without (CNTN2 KD) or with a contactin-2 rescue cDNA (KD + Rescue). Data shown are means  $\pm$  SEMs; number of cells (or fields of view for  $\text{Ca}^{2+}$  Spikes/Min)/independent cultures analyzed are depicted in the bars. Statistical significance was evaluated by Student's *t* test: \**P* < 0.05, \*\**P* < 0.01, \*\*\**P* < 0.001.

### CASPR2 KD Globally Decreases Synaptic Strength in a Cell-Autonomous Fashion.

Hypothesizing that the change in network activity induced by the CASPR2 KD may be attributable to a change in synaptic transmission, we next measured the size of evoked AMPA receptor (AMPA-R) and NMDA receptor (NMDA-R) mediated EPSCs and of GABA receptor-mediated inhibitory postsynaptic currents (IPSCs). The CASPR2 KD significantly decreased the amplitudes of all synaptic responses (Fig. 3A), without detectable changes in the subunit composition and/or voltage-dependent gating properties of postsynaptic receptors (Fig. S1A–D). Because the CASPR2 KD did not change the paired-pulse ratio of IPSCs (Fig. S1E and F), the decrease in synaptic responses was likely of postsynaptic origin. Consistent with an overall impairment in synaptic transmission, the frequency of spontaneous miniature (m)EPSCs and miniature (m)IPSCs was significantly decreased (Fig. 3B), with no decrease in the amplitude of mEPSCs but a small decrease in the amplitude of mIPSCs (Fig. S1G–J). Because CASPR2 is known to organize voltage-gated ion channels in axonal membrane subdomains in mature neurons (19, 27, 34–37), we asked whether the CASPR2 KD may produce the observed changes in synaptic transmission indirectly by altering the membrane properties of neurons. However, multiple indicators of neuronal excitability, including resting potential, action potential threshold, and spiking frequency in response to fixed current injections, were not affected by the CASPR2 KD, suggesting that the phenotype does not reflect a change in membrane properties (Fig. 3C and Fig. S2).

Because in our experiments, we knocked down CASPR2 by lentiviral delivery of shRNAs to all neurons in a culture, the phenotype could be attributable to either a presynaptic non-cell-autonomous effect, as indicated by the homology of CASPR2 to presynaptic neuroligins (20), or to a postsynaptic cell-autonomous effect. To address this question, we transfected isolated neurons with a control mCherry-expression vector, the KD vector coexpressing shRNAs with mCherry, or the KD vector coexpressing shRNAs with both mCherry and a rescue construct (Fig. 4A). We then patched neurons identified by mCherry fluorescence and monitored synaptic transmission by measuring evoked NMDA receptor-mediated responses (Fig. 4B). Similar to the effects of CASPR2 shRNA expression with lentiviruses, the CASPR2 KD in single neurons caused a large decrease in evoked synaptic responses, a significant decrease in mEPSC and mIPSC event frequency, and an additional decrease in neuronal capacitance but not input resistance (Fig. 4B–J). All of these changes were fully rescued by the CASPR2 cDNA (Fig. 4B–J).

### CASPR2 KD Impairs Dendritic Arbor and Spine Development.

The observation that the CASPR2 KD is equally effective in suppressing synaptic transmission upon delivery of shRNAs by lentiviruses or transfection indicates that the KD alters neuronal function postsynaptically in a cell-autonomous manner. However,

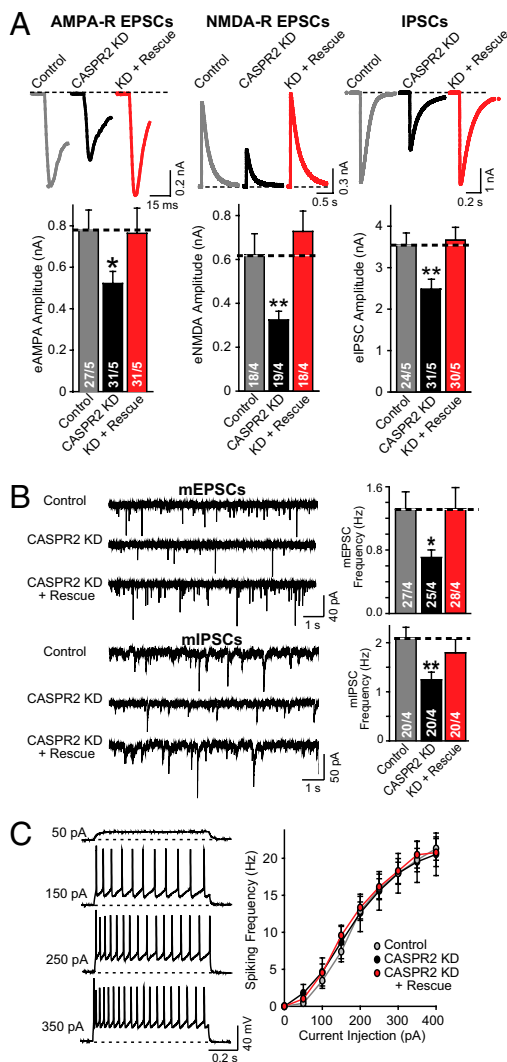


**Fig. 3.** CASPR2 KD decreases synaptic transmission without altering neuronal excitability. (A) Sample traces (*Upper*) and summary graphs of the amplitudes (*Lower*) of evoked NMDA-R- and AMPA-R-mediated EPSCs and of IPSCs as indicated, measured in neurons infected with control lentivirus (Control) or lentiviruses expressing the CASPR2 shRNA without (CASPR2 KD) or with a CASPR2 rescue cDNA (KD + Rescue). (B) Sample traces (*Left*) and frequency summary graphs (*Right*) of spontaneous miniature mEPSCs (*Upper*) or mIPSCs (*Lower*) measured in neurons infected with lentiviruses described in A, in the presence of 0.5  $\mu$ M tetrodotoxin. (C) Sample traces (*Left*) and spiking frequency summary graphs (*Right*) of action potentials induced by current injections in neurons obtained as described for A (see also Fig. S2). Data shown are means  $\pm$  SEMs; number of cells/independent cultures analyzed are depicted in the bars. Statistical significance was evaluated by Student's *t* test: \**P* < 0.05; \*\**P* < 0.01.

these data do not reveal whether the uniform decrease in synaptic transmission produced by the KD is caused by a change in synapse density, synapse function, and/or a decrease in the size of neurons resulting in an overall lowering in synapse numbers. To address this question, we analyzed neurons morphologically after KD of CASPR2 by transfection (Fig. 5) or lentiviral infection (Fig. S3).

Measurements of the total neurite length and neurite branching, both of which reflect the properties of dendrites, revealed that the KD of CASPR2 by transfection of single neurons (Fig. 5A–C) or by lentiviral infection of all neurons (Fig. S3C and D) produced a large decrease in dendritic arborization. No significant change in soma size was detected (Fig. 5D and Fig. S3D). The observed

decrease in the size of the dendritic arbor is consistent with the observed decrease in cell capacitance (Fig. 4C).

Analysis of the density and size of presynaptic specializations on neuronal dendrites from transfected control neurons and CASPR2 KD neurons, labeled using synapsin immunostaining, demonstrated that the CASPR2 KD produced no major change in synapse density or size (Fig. 5E–H and Fig. S3A and B). Moreover, examination of dendritic spines confirmed that the density of synapses was unchanged (Fig. 5I–K). Combined with the overall decrease in dendritic arborization observed in these neurons, this result indicates that the total number of synapses in a neuron is strongly reduced by the CASPR2 KD, which is also consistent with the decrease in mEPSC and mIPSC frequencies that is produced by the CASPR2 KD (Figs. 3B and 4E–J).

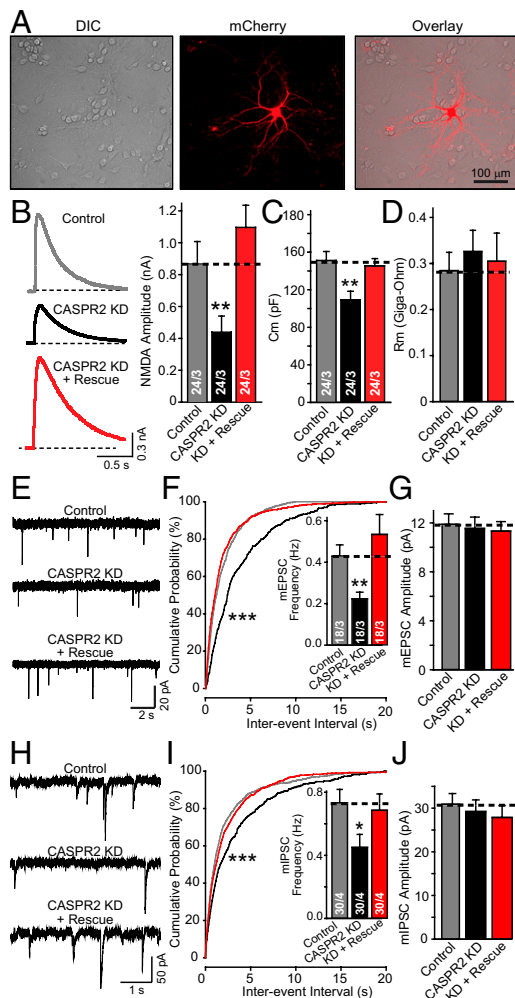


**Fig. 4.** CASPR2 KD acts cell-autonomously in impairing synaptic network activity. (A) Representative images of mCherry-expressing transfected neurons. (B) Sample traces (*Left*) and amplitude summary graphs (*Right*) of NMDA-R-mediated EPSCs evoked in neurons transfected with control mCherry-expressing vector (Control) or mCherry expression vector coexpressing the CASPR2 shRNA without (CASPR2 KD) or with a CASPR2 rescue cDNA (KD + Rescue). (C and D) Membrane capacitance (C) and input resistance (D) recorded from neurons described in B. (E–G) Sample traces of mEPSCs (E), cumulative plot of mEPSC interevent intervals (*Inset*, summary graph of event frequency) (F), and summary graph of averaged mEPSC amplitudes (G) recorded from neurons described in B. (H–J) Same as E–G, but for mIPSCs. Data shown are means  $\pm$  SEMs; number of cells/independent cultures analyzed are depicted in the bars. Statistical significance was evaluated by Student's *t* test (\**P* < 0.05; \*\**P* < 0.01) except for the cumulative probabilities that were analyzed by the Kolmogorov–Smirnov test (\*\*\**P* < 0.001).

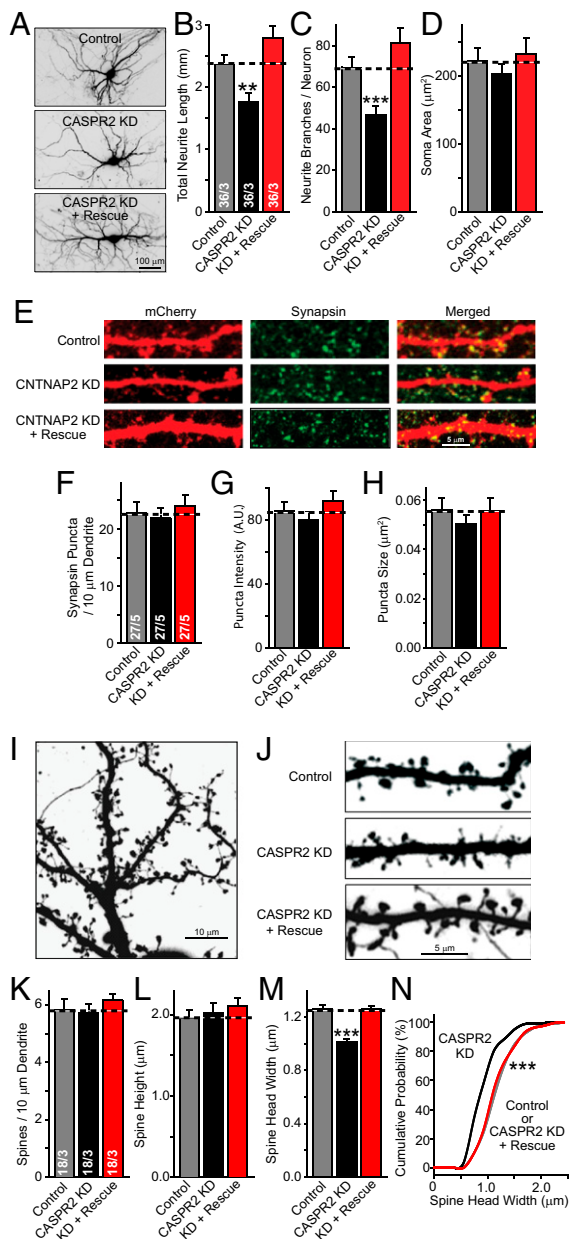


**Fig. 5.** CASPR2 KD impairs dendritic arbor and spine growth. (A–D) Representative images (A) and summary graphs of neuronal morphological properties [total dendritic length (B); dendritic branch points (C); somatic area (D)] of neurons transfected with control plasmid (Control) or plasmids expressing the CASPR2 shRNA without (CASPR2 KD) or with a CASPR2 rescue cDNA (KD + Rescue). (E–H) Representative images of dendrites of mCherry-expressing transfected neurons stained for synapsin (E) and summary graphs of the density (F), synapsin staining intensity (G), and size (H) of synapsin-positive puncta along a single dendrite. (I–N) Representative images of mCherry fluorescence in dendritic branches (I, magnified in J to visualize individual spines) and summary graphs of the density (K), average height (L) and head width (M) of spines along a single dendrite, and cumulative probability plots of the spine head width (N) in transfected neurons as described for A–D. Data shown are means  $\pm$  SEMs; number of cells/independent cultures analyzed are depicted in the bars. Statistical significance was evaluated by Student's *t* test (\* $P$  < 0.05; \*\* $P$  < 0.01; \*\*\* $P$  < 0.001) except for N, which was analyzed by the Kolmogorov–Smirnov test (\*\*\* $P$  < 0.001).

Further analysis of spine morphology revealed that although the CASPR2 KD left the height of spines unaltered (Fig. 5L), it significantly suppressed the width of the spine heads; again, this phenotype

was fully rescued by the CASPR2 cDNA (Fig. 5M). The decrease in spine head width was uniformly distributed across the entire spine population, suggesting that it was not attributable to an effect on a subpopulation of spines (Fig. 5N). Thus, the CASPR2 KD appears to impede the full development of dendritic specializations in a growing neuron, likely accounting for the deficits in global synaptic transmission that are observed upon the loss of CASPR2.

## Discussion

Previous studies revealed an essential role for CASPR2 in the assembly of the nodes of Ranvier in myelinated axons (27). Moreover, adult CASPR2 KO mice exhibited a 20% decrease in the number of inhibitory interneurons, a change in neuronal migration, epilepsy, altered  $\text{Ca}^{2+}$  oscillations in cortex, and behavioral abnormalities (26, 27). These results were of great interest because mutations in the human *CNTNAP2* gene encoding CASPR2 cause epilepsy and other neurological disorders, especially ASDs (for review, see ref. 4). Some of the diverse phenotypes of the CASPR2 KO mice, such as their epilepsy and behavioral abnormalities with a secondary loss of interneurons, could be potentially explained by the well-established function of CASPR2 as an organizer of axonal microdomains in myelinated nerves (reviewed in refs. 24 and 25). However, the changes in neuronal migration in CASPR2 KO mice are more consistent with a cell-autonomous role for CASPR2 earlier in development and cannot be easily explained by changes in the organization of axonal microdomains. Yet no function for CASPR2 outside of axonal microdomains has been directly demonstrated at present, even though this is a potentially important issue because ASD pathogenesis likely occurs before the maturation of myelinated axons. The present study attempts to address this apparent hole in our understanding by testing for a potential cell-autonomous role for CASPR2 in developing neurons.

Our results demonstrate that CASPR2 is required in a cell-autonomous fashion for the normal development of dendritic arbors and spines in excitatory neurons. Loss of CASPR2 causes a decrease in the total number of both excitatory and inhibitory synapses formed onto a neuron, resulting in an impairment of neural circuit assembly that manifests as a change in network activity. This phenotype agrees well with the observed changes in  $\text{Ca}^{2+}$  oscillations in CASPR2 KO mice in vivo (26). We observed a similar KD phenotype after delivery of shRNAs either by viral infection or by plasmid transfection and could fully rescue this KD phenotype by reexpression of shRNA-resistant CASPR2 cDNA, suggesting that the phenotype is specific. Moreover, we observed a strikingly different phenotype after KD of the CASPR2 ligand contactin-2, further documenting the specificity of the CASPR2 KD phenotype.

The cell-autonomous function of CASPR2 in dendritic development that we describe here acts early in development and is, thus, consistent with a neurodevelopmental pathogenesis of ASDs. Our study highlights the importance of CASPR2 in the architectural organization of the developing cortex, suggesting that CASPR2 performs a fundamental role in determining the structural patterning of cortical neurons. The consequence of CASPR2 dysfunction that results is abnormal neuronal circuit connectivity, which is a fundamental observation that likely plays a key role underlining the pathogenicity of genetic dysfunction in CASPR2 that is associated with ASDs.

Previous studies described direct or indirect protein interactions of CASPR2 that may provide insight into the mechanism of CASPR2 function in developing dendrites. In mature neurons, CASPR2 organizes a juxtaparanodal complex in the nodes of Ranvier by intracellular binding to protein 4.1 and MPP-type PDZ-domain proteins, which, in turn, recruit potassium channels and other proteins (38, 39). However, the effects of the CASPR2 KD on dendritic arborization are probably not mediated by changes in ion channel distribution that influence neuronal excitability because the CASPR2 KD did not change action potential generation (Fig. 3 and Fig. S2). Nevertheless, the binding of CASPR2 to protein 4.1 and other components of the juxtaparanodal complex may be important for dendritic arborization because such binding likely recruits other

elements of growing dendrites, in particular actin filaments, to cell-adhesion complexes mediated by CASPR2. Alternatively, CASPR2 may function by transducing an extracellular signal or by enabling another growth-factor receptor to transduce such a signal. Moreover, in *Drosophila* the CASPR2 homolog neurexin IV binds not only to contactins similar to its vertebrate counterpart (33) but also to other Ig-domain proteins such as neurofascin, wrapper, and roundabout (40–42). In addition, contactins bind to receptor phospho-tyrosine phosphatases (43, 44), which may mediate dendritic growth signaling via the protein tyrosine kinase fyn (45). Strikingly, our initial screen demonstrated that KD of the only known mammalian CASPR2 ligand, contactin-2, produces the opposite phenotype as the CASPR2 KD, a phenotype that can also be rescued with wild-type contactin-2 (Fig. 2). This result suggests that the cell-autonomous dendritic function of CASPR2 operates via a ligand interaction that is in competition with CASPR2-binding to contactin-2 and, thus, activated by the contactin-2 KD. Identifying this ligand, which may be one of the several neurexin IV ligands identified in *Drosophila*, will be of paramount importance and will potentially provide further insights into the role of CASPR2 in ASD pathogenesis.

Independent of the detailed molecular mechanisms by which CASPR2 acts, this study identifies a cell-autonomous function for CASPR2 in controlling the growth of dendritic arbors and spines before myelination. The CASPR2 function we describe here suggests a mechanism by which CASPR2 mutations could influence the assembly of neural circuits and provides a plausible hypothesis for the role of these mutations in the pathogenesis of ASDs.

## Methods

Briefly, shRNAs to candidate ASD synaptic cell adhesion proteins and rescue constructs were expressed in cortical neurons cultured from P0 CD1 mice on DIV 4 using lentiviruses or calcium-phosphate transfection. Ca<sup>2+</sup> imaging of network activity as well as electrophysiological and morphological measurements were made 10–14 d after shRNA delivery. For a detailed description of methods, see *SI Methods*.

**ACKNOWLEDGMENTS.** This study was supported by National Institute of Mental Health Grants MH052804 and MH089054 and National Institute of Neurological Disorders and Stroke Grant R01 NS077906. G.R.A. is supported by National Institutes of Health Training Grant 2T32 NS007280-26A1 and Autism Speaks Translational Postdoctoral Fellowship Grant 7953. J.A. is supported by American Heart Association Award 11POST7360078.

- Holt R, Monaco AP (2011) Links between genetics and pathophysiology in the autism spectrum disorders. *EMBO Mol Med* 3(8):438–450.
- State MW, Levitt P (2011) The conundrums of understanding genetic risks for autism spectrum disorders. *Nat Neurosci* 14(12):1499–1506.
- Persico AM, Bourgeron T (2006) Searching for ways out of the autism maze: Genetic, epigenetic and environmental clues. *Trends Neurosci* 29(7):349–358.
- Peñagarikano O, Geschwind DH (2012) What does CNTNAP2 reveal about autism spectrum disorder? *Trends Mol Med* 18(3):156–163.
- Friedman JL, et al. (2008) CNTNAP2 gene dosage variation is associated with schizophrenia and epilepsy. *Mol Psychiatry* 13(3):261–266.
- Mefford HC, et al. (2010) Genome-wide copy number variation in epilepsy: Novel susceptibility loci in idiopathic generalized and focal epilepsies. *PLoS Genet* 6(5):e1000962.
- Strauss KA, et al. (2006) Recessive symptomatic focal epilepsy and mutant contactin-associated protein-like 2. *N Engl J Med* 354(13):1370–1377.
- Belloso JM, et al. (2007) Disruption of the CNTNAP2 gene in a t(7;15) translocation family without symptoms of Gilles de la Tourette syndrome. *Eur J Hum Genet* 15(6):711–713.
- Verkerk AJ, et al.; Tourette Syndrome Association International Consortium for Genetics (2003) CNTNAP2 is disrupted in a family with Gilles de la Tourette syndrome and obsessive compulsive disorder. *Genomics* 82(1):1–9.
- O'Dushlaine C, et al. (2011) Molecular pathways involved in neuronal cell-adhesion and membrane scaffolding contribute to schizophrenia and bipolar disorder susceptibility. *Mol Psychiatry* 16(3):286–292.
- Elia J, et al. (2010) Rare structural variants found in attention-deficit hyperactivity disorder are preferentially associated with neurodevelopmental genes. *Mol Psychiatry* 15(6):637–646.
- Zweier C, et al. (2009) CNTNAP2 and NRXN1 are mutated in autosomal-recessive Pitt-Hopkins-like mental retardation and determine the level of a common synaptic protein in *Drosophila*. *Am J Hum Genet* 85(5):655–666.
- Sehested LT, et al. (2010) Deletion of 7q34-q36.2 in two siblings with mental retardation, language delay, primary amenorrhea, and dysmorphic features. *Am J Med Genet A* 152A(12):3115–3119.
- Vernes SC, et al. (2008) A functional genetic link between distinct developmental language disorders. *N Engl J Med* 359(22):2337–2345.
- Newbury DF, Monaco AP (2010) Genetic advances in the study of speech and language disorders. *Neuron* 68(2):309–320.
- Petrin AL, et al. (2010) Identification of a microdeletion at the 7q33-q35 disrupting the CNTNAP2 gene in a Brazilian stuttering case. *Am J Med Genet A* 152A(12):3164–3172.
- Tan GC, Doke TF, Ashburner J, Wood NW, Frackowiak RS (2010) Normal variation in fronto-occipital circuitry and cerebellar structure with an autism-associated polymorphism of CNTNAP2. *Neuroimage* 53(3):1030–1042.
- Scott-Van Zeeland AA, et al. (2010) Altered functional connectivity in frontal lobe circuits is associated with variation in the autism risk gene CNTNAP2. *Sci Transl Med* 2(56):56ra80.
- Poliak S, et al. (1999) Caspr2, a new member of the neurexin superfamily, is localized at the juxtaparanodes of myelinated axons and associates with K<sup>+</sup> channels. *Neuron* 24(4):1037–1047.
- Südhof TC (2008) Neuroligins and neurexins link synaptic function to cognitive disease. *Nature* 455(7215):903–911.
- Sanders SJ, et al. (2011) Multiple recurrent de novo CNVs, including duplications of the 7q11.23 Williams syndrome region, are strongly associated with autism. *Neuron* 70(5):863–885.
- Kim HG, et al. (2008) Disruption of neurexin 1 associated with autism spectrum disorder. *Am J Hum Genet* 82(1):199–207.
- Levy D, et al. (2011) Rare de novo and transmitted copy-number variation in autistic spectrum disorders. *Neuron* 70(5):886–897.
- Peles E, Salzer JL (2000) Molecular domains of myelinated axons. *Curr Opin Neurobiol* 10(5):558–565.
- Girault JA, Oguevetskaia K, Carnaud M, Denisenko-Nehrbass N, Goutebroze L (2003) Transmembrane scaffolding proteins in the formation and stability of nodes of Ranvier. *Biol Cell* 95(7):447–452.
- Peñagarikano O, et al. (2011) Absence of CNTNAP2 leads to epilepsy, neuronal migration abnormalities, and core autism-related deficits. *Cell* 147(1):235–246.
- Poliak S, et al. (2003) Juxtaparanodal clustering of Shaker-like K<sup>+</sup> channels in myelinated axons depends on Caspr2 and TAG-1. *J Cell Biol* 162(6):1149–1160.
- Xu W, et al. (2012) Distinct neuronal coding schemes in memory revealed by selective erasure of fast synchronous synaptic transmission. *Neuron* 73(5):990–1001.
- Kaesler PS, et al. (2011) RIM proteins tether Ca<sup>2+</sup> channels to presynaptic active zones via a direct PDZ-domain interaction. *Cell* 144(2):282–295.
- Geppert M, et al. (1994) Synaptotagmin I: A major Ca<sup>2+</sup> sensor for transmitter release at a central synapse. *Cell* 79(4):717–727.
- Gunnarsen JM, et al. (2007) Seiz-6 proteins affect dendritic arborization patterns and excitability of cortical pyramidal neurons. *Neuron* 56(4):621–639.
- Alvarez VA, Ridenour DA, Sabatini BL (2006) Retraction of synapses and dendritic spines induced by off-target effects of RNA interference. *J Neurosci* 26(30):7820–7825.
- Peles E, et al. (1997) Identification of a novel contactin-associated transmembrane receptor with multiple domains implicated in protein-protein interactions. *EMBO J* 16(5):978–988.
- Einheber S, et al. (1997) The axonal membrane protein Caspr, a homologue of neurexin IV, is a component of the septate-like paranodal junctions that assemble during myelination. *J Cell Biol* 139(6):1495–1506.
- Menegoz M, et al. (1997) Paranodin, a glycoprotein of neuronal paranodal membranes. *Neuron* 19(2):319–331.
- Traka M, et al. (2003) Association of TAG-1 with Caspr2 is essential for the molecular organization of juxtaparanodal regions of myelinated fibers. *J Cell Biol* 162(6):1161–1172.
- Inda MC, DeFelipe J, Muñoz A (2006) Voltage-gated ion channels in the axon initial segment of human cortical pyramidal cells and their relationship with chandelier cells. *Proc Natl Acad Sci USA* 103(8):2920–2925.
- Horresher I, Bar V, Kissil JL, Peles E (2010) Organization of myelinated axons by Caspr and Caspr2 requires the cytoskeletal adapter protein 4.1B. *J Neurosci* 30(7):2480–2489.
- Horresher I, et al. (2008) Multiple molecular interactions determine the clustering of Caspr2 and Kv1 channels in myelinated axons. *J Neurosci* 28(52):14213–14222.
- Charles P, et al. (2002) Neurofascin is a glial receptor for the paranodin/Caspr-contactin axonal complex at the axoglial junction. *Curr Biol* 12(3):217–220.
- Stork T, et al. (2009) *Drosophila* Neurexin IV stabilizes neuron-glia interactions at the CNS midline by binding to Wrapper. *Development* 136(8):1251–1261.
- Banerjee S, et al. (2010) *Drosophila* neurexin IV interacts with Roundabout and is required for repulsive midline axon guidance. *J Neurosci* 30(16):5653–5667.
- Peles E, et al. (1995) The carbonic anhydrase domain of receptor tyrosine phosphatase beta is a functional ligand for the axonal cell recognition molecule contactin. *Cell* 82(2):251–260.
- Milev P, Maurel P, Häring M, Margolis RK, Margolis RU (1996) TAG-1/axonin-1 is a high-affinity ligand of neurocan, phosphacan/protein-tyrosine phosphatase-zeta/beta, and N-CAM. *J Biol Chem* 271(26):15716–15723.
- Zeng L, D'Alessandri L, Kalousek MB, Vaughan L, Pallen CJ (1999) Protein tyrosine phosphatase alpha (PTPalph) and contactin form a novel neuronal receptor complex linked to the intracellular tyrosine kinase fyn. *J Cell Biol* 147(4):707–714.